A porous silicon Bragg grating waveguide by direct laser writing

2008 J. Phys.: Condens. Matter 20 365203

(http://iopscience.iop.org/0953-8984/20/36/365203)

J. Phys.: Condens. Matter **20** (2008) 365203 (4pp) doi:10.1088/0953-8984/20/36/365203

A porous silicon Bragg grating waveguide by direct laser writing

Ilaria Rea[1,2], Antigone Marino[2], Mario Iodice[1], Giuseppe Coppola[1], Ivo Rendina[1] and Luca De Stefano[1]

[1] National Council of Research, Institute for Microelectronic and Microsystems, Department of Naples, Via P Castellino 111, I-80131 Naples, Italy
[2] Department of Physics, 'Federico II' University of Naples, Via Cinthia, I-80126 Naples, Italy

E-mail: ilaria.rea@na.imm.cnr.it

Received 9 May 2008, in final form 24 July 2008
Published 12 August 2008
Online at stacks.iop.org/JPhysCM/20/365203

Abstract
We have designed, fabricated and characterized a porous silicon-based Bragg grating integrated in an optical waveguide, by using a low cost and fast technique, direct laser writing. A periodic optical structure with a pitch of 10 μm, resonant in the near-infrared wavelength region, has been obtained. The simulated transmission spectra, calculated by the transfer matrix method and waveguide modal computation, are in good qualitative agreement with the experimental ones. The waveguide transmission losses have been quantified as 22 dB cm^{-1}.

1. Introduction

Porous silicon (PSi) is one of the most exciting materials for silicon-based optoelectronics: its morphological and physical properties allow the fabrication of a huge variety of photonic devices with a single computer-controlled electrochemical process. By modulating the porosity of PSi layers and their spatial succession, optical resonant structures, such as optical microcavities [1] and quasi-periodic Thue–Morse sequences [2], but also photonic crystals from the simple 1D to the very complex 3D, can be obtained [3]. Most of these devices find their killer application in the optical sensing field rather than in optical telecommunications. Even if the PSi technology is almost compatible with standard integrated circuit technologies, the utilization of photolithography is rather difficult: the masking process by photoresist deposition is not fit for PSi, since the polymers used show a low resistance to the acid solutions used during the electrochemical process. On the other hand, PSi is rapidly etched by alkaline solutions used as developers of photoresists. The direct laser writing (DLW) is thus a patterning process alternative to the traditional photolithographic approach which exploits the ablation–oxidation of the PSi surface, induced by a blue laser. This powerful technique has recently been used in the direct writing of micropatterns on the PSi surface [4] in order to define channel waveguides [5, 6] or oxidized regions for selective cell growth [7]. Due to the low thermal conductivity of the PSi, the high temperature necessary for the writing process (about 900 °C) can be obtained by a low power laser [8].

In this work, we have used the DLW process to etch a high-order Bragg grating on a PSi slab waveguide, obtaining a resonant structure in the near-infrared which has been characterized by end-fire coupling. Bragg grating optical filters photoinduced in waveguides are cost-effective devices for applications in optical networks, waveguide lasers and optical sensors. Bragg gratings in silica planar waveguides increase the versatility of planar lightwave circuits which already have the advantage of being compatible with well-established semiconductor processing technologies. Lots of photonic devices—such as wavelength division multiplexers, photonic beam-formers, external-cavity lasers and optical sensors that measure the refractive index of their surroundings—all benefit from the incorporation of Bragg grating technology [9]. One of the challenges for devices with integrated Bragg gratings is the ease of their fabrication, but also the regularity of their geometrical features. We would like to underline that, even if some submicrometer gratings have been fabricated on PSi surfaces by electron beam (EB) lithography or direct writing, not one of these structures has been optically characterized [6]. Moreover, DLW requires much simpler and less expensive equipment with respect to EB.

2. Materials and methods

A highly doped p$^+$-silicon, ⟨100⟩ oriented, 0.01 Ω cm resistivity, 400 μm thick was used as the substrate in

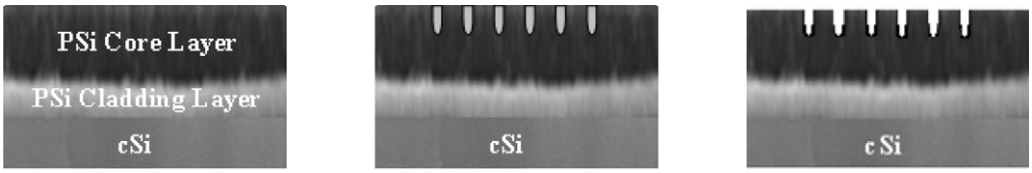

(A) (B) (C)

Figure 1. PSi-based BGW fabrication process flowchart.

the PSi Bragg grating waveguide (BGW) fabrication. The slab waveguide was obtained by electrochemical etching of crystalline silicon in an HF-based solution (50 wt% HF:ethanol = 3:7) in the dark and at room temperature. Since the Psi fabrication process is self-stopping, it is possible to make adjacent layers with different porosities by changing the current during the process [10]. A current density of 10 mA cm^{-2} was applied for 18.9 s to produce the core layer of thickness 2.5 μm and porosity 65%, while a current density of 109 mA cm^{-2} was applied for 13.6 s in the case of the cladding layer with thickness 2.5 μm and porosity 78%, as is shown in the flow process reported in figure 1(A), where the PSi asymmetric slab waveguide is depicted. These porosities correspond to core and cladding refractive indexes of 1.65 and 1.52, respectively, calculated by the Bruggeman model [11] at a wavelength of 1.5 μm.

Thicknesses and porosities of the porous silicon layers have been estimated by variable angle spectroscopic ellipsometry (UVISEL, Horiba, Jobin–Yvon). After the electrochemical etching, the sample was rinsed in ethanol and dried under a stream of N_2. A 50-period BGW was written on the porous surface of the upper layer by laser ablation/oxidation using a 406 nm wavelength laser diode beam (spot diameter $\approx$ 1.5 mm) at normal incidence, focused by a 40$\times$ (NA = 0.65) microscope objective (figure 1(B)). The sample was mounted on a motorized x–y micrometric stage (Micos LS-110) and scanned at a speed of 0.01 mm s^{-1}. More details on the laser writing process can be found elsewhere [12]. After the writing process, we removed the oxidized region by rinsing the PSi structure in a low concentration HF-based solution for 10 s, as is shown in figure 1(C).

The device was then fully oxidized in pure O_2 by a two-step thermal treatment (400 °C for 30 min and 900 °C for 15 min). The oxidation strongly reduces the roughness of the interfaces and, as a consequence, the scattering losses of the waveguide [13].

The last fabrication step was the cleaving of the waveguide edges in a direction parallel to the grating in order to allow the measurement of the BGW transmission spectrum by end-fire fiber coupling.

The morphological characteristics of the Bragg grating were investigated by scanning electron microscopy using a field emission instrument Zeiss SUPRA.

The core and cladding refractive indices of the oxidized PSi waveguide were measured by the standard m-line method [14] at 1.55 μm in TE polarization. The transmission spectral response of the BGW was registered by end-fire coupling. A sweeping tunable laser source (Ando AQ4321D) was launched into the waveguide by a single-mode lensed fiber; a second fiber collected the light at the end of the device and sent the signal to an optical spectrum analyzer (Ando AQ6317C) synchronized with the tunable laser source. The spectrum was acquired in the wavelength range of 1520–1620 nm with a resolution of 0.1 nm. The waveguide optical losses were measured by analyzing the scattered light from the top surface [15, 16]. A laser beam at 1.55 μm was coupled into the waveguide by a single-mode lensed fiber and the upper out-of-plane scattered light intensity was recorded by an infrared CCD camera (Xenics Xeva) placed above the structure.

3. Experimental results and discussion

In figures 2(A) and (B) we report two electronic microscope images of the PSi Bragg grating waveguide after HF rinsing and thermal oxidation: figure 2(A) shows very regular air trenches etched by laser light in the porous silicon surface: the grating pitch Λ is about 10 μm and the duty cycle is about 0.7.

Figure 2(B) is a detail of a single-element end: quite regular walls with a porosity gradient along the vertical direction can be observed. The whole structure is extended on an area of about 0.7 mm^2 and consists of 1.3 mm long straight lines, perpendicular to the propagation direction. The depth profile of the Bragg grating, as measured by the profilometer (Tencor P15), is shown in figure 3. The typical V-shaped trenches, due to an inhomogeneous thermal distribution during the laser etching and already observed by Rossi and coworkers [5], are 1 μm deep and have a full width at half-maximum of 3 μm.

The oxidized PSi waveguide has been characterized before the laser writing process by m-lines spectroscopy in order to measure the core and cladding refractive index [14]. We obtained a value of 1.361 $\pm$ 0.001 for the core refractive index and of 1.18 $\pm$ 0.01 for the cladding. From these values, the effective refractive indices $n_{\mathrm{eff},m}$ of the fundamental (m = 0) and first vertical mode (m = 1), supported by the slab waveguide, were estimated to be 1.341 and 1.282, respectively [15]. We have characterized the PSi waveguide optical losses by measuring the light scattered from the top surface. In fact, if we assume a constant scattering mechanism along the structure, the scattered intensity in the vertical direction is proportional to the intensity of the guided light [16]. Figure 4 shows a top view image of the scattered light from the device registered by an infrared camera: it is very clear that the beam diverges and its intensity decreases along the propagation direction. The losses are measured along the light propagation direction in a region containing

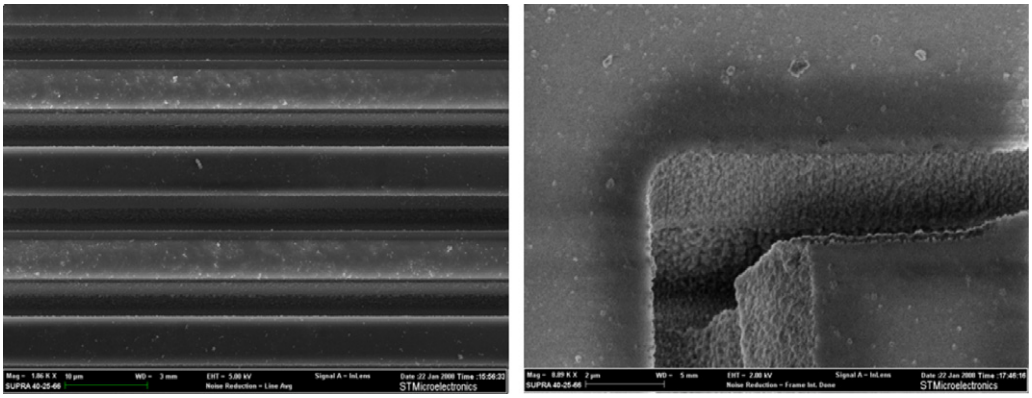

(A) (B)

Figure 2. (A) SEM top view of the BGW structure. (B) Detail of a single-element end.

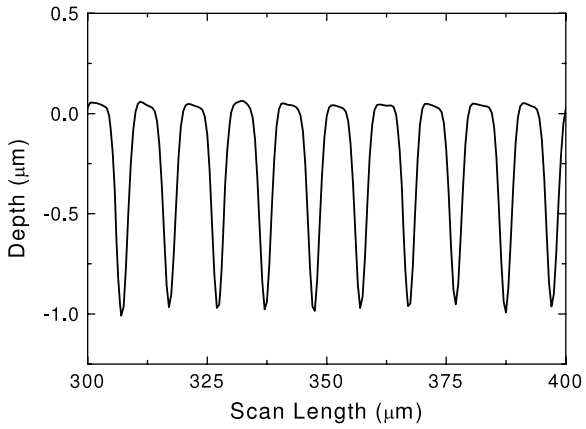

Figure 3. Thickness profile of the BGW measured by the profilometer after HF rinsing.

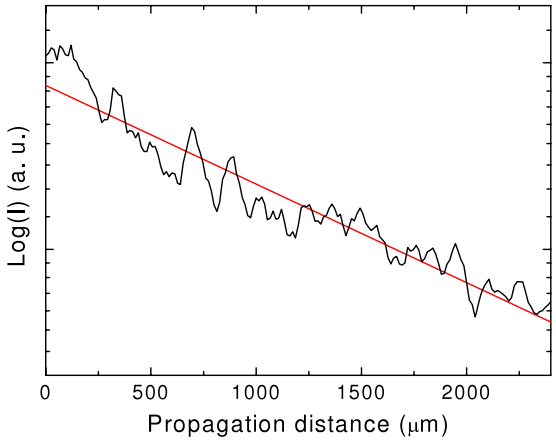

Figure 5. Top view of the scattered light from the surface of the oxidized PSi waveguide at $\lambda = 1.55$ μm.

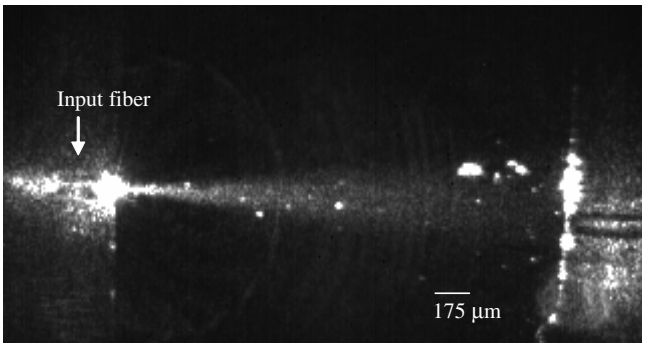

Figure 4. Top view of the scattered light from the surface of the oxidized PSi waveguide at 1.55 μm.

the luminous streak but excluding the defect scattering centers: an exponential decreasing behavior of the light intensity was observed. If we report in logarithmic scale the optical signal registered as a function of the propagation distance, as can be seen in figure 5, we can estimate the light attenuation by the slope of this curve.

The conversion in dB cm^{-1} of this number gives an estimated value of the losses equal to 22.3 ± 0.9 dB cm^{-1}, in agreement with that reported in the literature [17, 18].

The Bragg grating can be considered as a periodic perturbation of the waveguide which forbids the forward propagation of the electromagnetic radiation at specific wavelengths, according to the condition $\lambda_B = 2n_{eff}\Lambda$, where λ_B is the Bragg wavelength, n_{eff} the effective refractive index of the mode supported by the waveguide and Λ the grating pitch. To obtain such an optical gap in the near-infrared region, the pitch should be of the order of a few hundred nanometers, close to the resolution of standard technologies used in integrated circuits. The porous silicon walls should also be too thin (about 500 nm) to be safely handled [19]. To overcome these problems, high-order Bragg gratings could be considered: in this case, the resonance condition becomes $\lambda_B = 2n_{eff}\Lambda/k$, where k is an integer called the order of the Bragg grating and which represents the number of quarter-wavelengths within the air and porous silicon refractive indexes.

The transmission spectrum of the resonant structure can be calculated by using the transfer matrix method together with the slab waveguide modal calculation [15]. In figure 6 we show the experimental (solid curve) and calculated (dash curve) transmission spectra of the PSi BGW: there is a good qualitative agreement between the two spectra. The

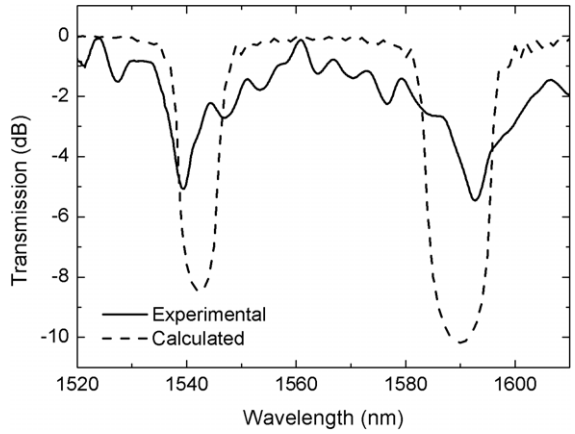

Figure 6. Experimental (solid curve) and calculated (dash curve) transmission spectra of the BGW structure.

transmission peaks, present at 1540 nm and 1590 nm, correspond to the seventeenth Bragg order of the fundamental guided mode and the sixteenth Bragg order of the first guided mode, respectively. The oscillations of the baseline between the two peaks can be attributed to the inner surface roughness and variation of the wall thicknesses due to the DLW fabrication process [20]. The contrast reduction in the transmitted intensity between the numerical and experimental spectra is about 4 dB and due to the scattering losses experienced by the propagating modes in the PSi slab waveguide.

4. Conclusions

In conclusion, the laser direct writing of a resonant structure in a PSi-based slab waveguide has been demonstrated by fabricating a high-order Bragg grating. The structure, with a pitch of 10 μm, has been optically characterized. The experimental transmission spectrum of the BGW has been compared with the calculated one. The agreement between the spectra is a demonstration of the good control in the fabrication process, suggesting the possibility to use the PSi BGW as an optical sensor of biochemical substances and in lab-on-chip applications. Even if the optical losses can be reduced by proper design below an acceptable value for telecommunication purposes, for example under 1 dB cm^{-1} as reported in the recent literature [5, 17], we believe that the ultimate application of such a device can be in chemical and biological sensing. The ease and low cost of fabrication, together with the morphological features of porous silica, can be key factors for successful sensor devices.

Acknowledgment

The authors gratefully acknowledge Dr N Malagnino of STMicroelectronics for SEM images.

References

[1] Mulloni V and Pavesi L 2000 *Appl. Phys. Lett.* **76** 2523
[2] Moretti L, Rea I, Rotiroti L, Rendina I, Abbate G, Marino A and De Stefano L 2006 *Opt. Express* **14** 6264–72
[3] Birner A, Wehrspohn R B, Gösele U M and Busch K 2001 *Adv. Mater.* **13** 377–88
[4] Park H, Dickerson J H and Weiss S M 2008 *Appl. Phys. Lett.* **92** 011113
[5] Rossi M, Amato G, Camarchia V, Boarino L and Borini S 2001 *Appl. Phys. Lett.* **78** 3003–5
[6] Rossi M, Borini S, Boarino L and Amato G 2003 *Phys. Status Solidi* a **197** 284–7
[7] Khung Y, Graney S D and Voelcker N H 2006 *Biotechnol. Prog.* **22** 1388–93
[8] Timoshenko V Y, Dittrich T, Sieber I, Rappich J, Kamenev B V and Kashkarov P K 2000 *Phys. Status Solidi* a **182** 325
[9] Dai X, Mihailov S J and Walker R 2006 *Meas. Sci. Technol.* **17** 1752–6
[10] Lehman V 2002 *Electrochemistry of Silicon* (New York: Wiley–VCH) pp 17–20
[11] Hardeman R W, Beale M I J, Gasson D B, Keen J M, Pickering C and Robbins D J 1985 *Surf. Sci.* **152/153** 1051–62
[12] De Stefano L, Rea I, Della Corte F G, Nigro M A and Rendina I 2008 *J. Phys.: Condens. Matter* **20** 265009
[13] Pap E, Kordás K, Tóth G, Levoska J, Uusimäki A, Vähäkangas J, Leppävuori S and George T F 2005 *Appl. Phys. Lett.* **86** 041501
[14] Ding T N and Garmire E 1983 *Appl. Opt.* **22** 3177–81
[15] Kogelnik H 1979 *Integrated Optics* 2nd edn, ed T Tamir (New York: Springer)
[16] Channin D J, Hammer J M and Duffy M T 1975 *Appl. Opt.* **14** 923–30
[17] Pirasteh P, Charrier J, Dumeige Y, Haesaert S and Joubert P 2007 *J. Appl. Phys.* **101** 083110
[18] Arrand H F, Benson T M, Loni A, Arens-Fischer R, Krüger M, Thönissen M, Lüth K and Kershaw S 1998 *IEEE Photon. Technol. Lett.* **10** 1467–9
[19] Barillaro G, Diligenti A, Benedetti M and Merlo S 2006 *Appl. Phys. Lett.* **89** 151110
[20] Barillaro G, Annovazzi-Lodi V, Benedetti M and Merlo S 2007 *Appl. Phys. Lett.* **90** 121110